Rapid Communication

J. Biochem. 2009;146(5)627–631
doi:10.1093/jb/mvp121

Vimentin Intermediate Filaments as a Template for Silica Nanotube Preparation

Rumi Gohara[1], Dian Liu[2], Kenichi Nakashima[2], Yozo Takasaki[1] and Shoji Ando[1,*]

[1]Department of Biomolecular Sciences, Faculty of Medicine, Saga University, Nabeshima, Saga 849-8501; and [2]Department of Chemistry, Faculty of Science and Engineering, Saga University, Honjo-machi, Saga 840-8502, Japan

Received July 8, 2009; accepted July 25, 2009; published online August 5, 2009

Organic compounds are used as templates to regulate the morphology of inorganic nanostructures. In the present study, we used intermediate filaments (IFs), the major cytoskeleton component of most eukaryotic cells, as a template for hollow silica nanotube preparation. Sol–gel polymerization of tetraethoxysilane proceeded preferentially on the surface of IFs assembled from vimentin protein *in vitro*, resulting in silica-coated fibres. After removing IFs by calcination, electron microscopy revealed hollow silica nanotubes several micrometers long, with outer diameters of 35–55 nm and an average inner diameter of 10 nm (comparable to that of IFs). Furthermore, the silica nanotubes exhibited a gnarled surface structure with an 18–26 nm repeating pattern (comparable to the 21-nm beading pattern along IFs). Thus, the characteristic morphology of IFs were well replicated into hollow silica nanotubes, suggesting that IFs maybe useful as an organic template.

Key words: intermediate filaments, nanotube, silica, sol–gel polymerization, vimentin.

Abbreviations: AFM, atomic force microscopy; IF, intermediate filament; TEM, transmission electron microscopy; TEOS, tetraethoxysilane.

The creation of precisely controlled inorganic structures at a nanometer scale is of considerable interest for use as catalysts, nanowires, circuits, molecular containers and complicated patterning required in nanotechnology applications (*1–3*). However, inorganic compounds generally lack the ability to self-assemble into nanostructures with regulated morphology. By contrast, natural or designed organic molecules exhibit those characteristics under appropriate conditions, and organic structures with diverse and well-regulated shapes have been used as templates onto which inorganic materials can be deposited (*3–6*). For instance, inorganic structures including fibres, tubules or spheres of silica (SiO_2), titania (TiO_2) and other common oxides have been created using organic templates such as synthetic polymers, surfactants, proteins and DNAs (*4*, *6*). Silica nanostructures, in particular, have great potential for use in catalysis and electronics applications, and the sol–gel chemistry of silica, in which tetraalkoxysilicate precursors are hydrolysed and condensed through the interaction with cationic charges of organic templates, has been extensively studied (*3*, *4*, *6*). Nanostructures of silica have been synthesized by this method using organic templates such as phospholipids (*7*), peptidic lipid (*8*), laurylamine hydrochloride (*9*), collagen fibres (*10*), DNAs (*11*), peptide fibrils (*12*, *13*) and polymeric micelles (*14*).

Intermediate filaments (IFs), a major component of the cytoskeleton of most eukaryotic cells, are attractive candidates for an organic template as their filament structures (several micrometer lengths and a uniform 10-nm diameter) are easily constructed *in vitro* by polymerization of subunit proteins without any cofactors, and they are very stable compared with other cytoskeletal components such as actin filaments and microtubules (*15–18*). In addition, IFs form large fibres or macrofibrils in which many are highly aligned in parallel arrays through the interaction with IF-associated proteins (*19*). Neuron-specific IFs (neurofilaments) create fibrous networks that are extensively cross-linked to each other by lateral cross-bridges formed by various linking proteins and the extended domains of the neurofilament proteins (*20*), while nuclear lamin IFs in nuclear lamina exhibit a marked near-tetragonal meshwork that lines the inner nuclear membrane (*16*, *21*).

The genes encoding IF proteins are well characterized in vertebrates; in humans 70 distinct genes have been described (*22*). All IF proteins share a characteristic tripartite structure that includes the central α-helical rod domain flanked by the non-α-helical N-terminal head and C-terminal tail domains (*16-18*). The rod domain, consisting of ~310 amino acids, has relatively conserved sequences at the N- and C-terminal ends, and displays long heptad-repeat patterns (*abcdefg*) of hydrophobic residues (*a* and *d*). The rod domain is responsible for the initial association of IF proteins into a coiled-coil dimer and also for higher-order polymerization into IFs. The rod domains pack closely together to form the backbone of IFs, with the head and tail domains lying largely on the surface (*16–18*). In contrast to the rod domain, the both end domains of individual IF proteins are extremely

*To whom correspondence should be addressed. Tel: +81-952-34-2192, Fax: +81-952-34-2418, E-mail: andohs@cc.saga-u.ac.jp

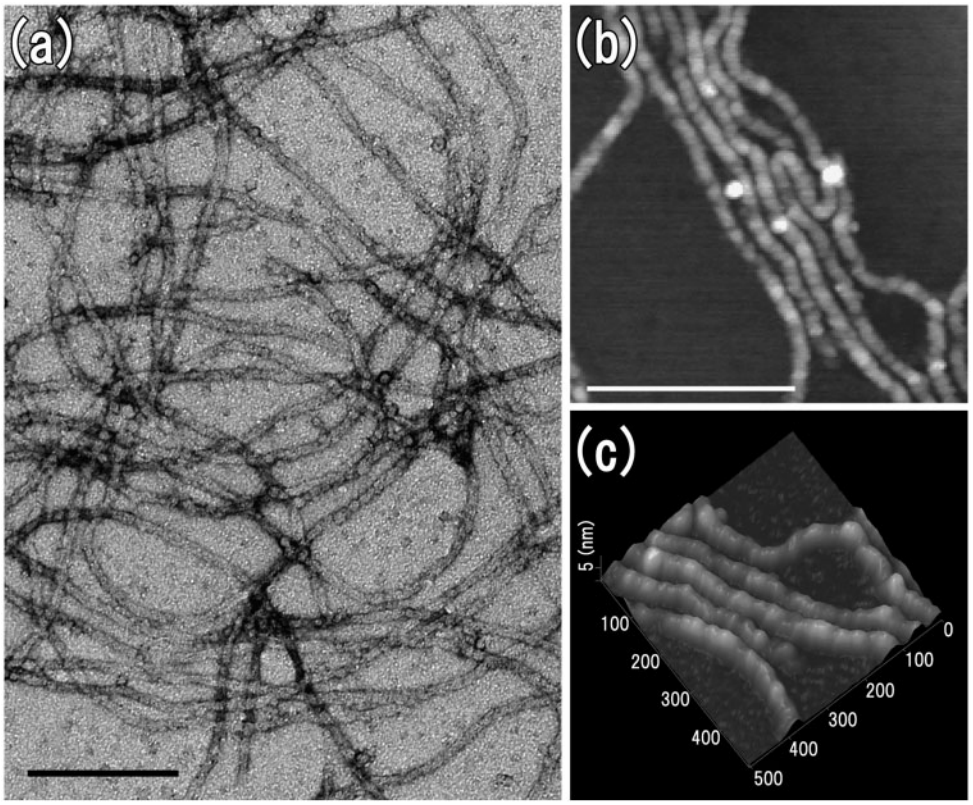

Fig. 1. **Negative-staining TEM (a) and AFM (b and c) images of vimentin IFs.** (a) Vimentin IFs constructed *in vitro* were dropped on specimen grids, the excess solution drained by touching filter paper after 3 min, and then negatively stained with 2% uranyl acetate. The AFM image (b) was processed computationally into the 3D image (c). The images (b) and (c) show the 21-nm beading pattern along vimentin IFs. Scale bars represent 200 nm in (a) and 500 nm in (b).

variable both in size and amino acid sequence, and are primarily responsible for determining the unique characteristics of the individual IF proteins.

In the present study, we examined competence of vimentin IFs as a template for preparation of hollow silica nanotubes. Vimentin is a typical IF protein expressed in mesenchymal cells, and the *in vitro* assembly conditions required for vimentin IF production have been established (*16–18*, *23*). As the head domain of vimentin is very basic, due to a wealth of arginine residues, and is considered to be located on the surface of vimentin IFs, we hypothesized that the cationic charges of the head domain play a crucial role in silica mineralization around vimentin IFs.

Mouse vimentin (57 kDa) was produced by bacterial expression using pET3a vector and isopropyl-β-D-thiogalactopyranoside induction, and then purified by ion-exchange column chromatography on Q- and SP-Sepharose resin, as previously described (*23*). The purified vimentin was dialyzed against a high pH buffer (buffer A: 10 mM Tris–HCl, pH 8.8, 2 mM EDTA, 10 mM 2-mercaptoethanol), and cleared of aggregates by centrifugation at 100,000*g* for 1 h at 4°C. The protein concentration was determined by the Bradford method (*24*), using bovine serum albumin as a standard.

In a high pH and low ionic strength buffer, soluble vimentin was reported to start assembly into IFs immediately after adjusting to physiological pH and ionic strength (*17*, *23*). In the present study, IF assembly of vimentin was initiated by addition of soluble vimentin (6.0 mg/ml) in buffer A to 30 vol of buffer B (10 mM imidazole–HCl, pH 7.2, 150 mM NaCl, 2 mM 2-mercaptoethanol). Using this dilution, vimentin usually forms typical IFs ~10 nm in diameter of several micrometers long within 1 h (Fig. 1a), as observed by transmission electron microscopy (TEM) under a JEM-1210 electron microscope (JEOL, Tokyo, Japan) at 80 kV after negative staining. Furthermore, vimentin IFs exhibit the 21-nm beading pattern along the filament axis (Fig. 1b and c), as observed by atomic force microscopy (AFM) in the dynamic force mode under an SPA 300 unit together with a SPI 3700 control station (SII, Chiba, Japan) (*23*). The characteristic 21-nm beading pattern of IFs has been also observed by rotary-shadowing electron microscopy (*25*, *26*) and freeze-etch electron microscopy (*27*). Immediately after initiation of IF assembly by dilution, the vimentin solution was mixed with 3 vol of 200 mM tetraethoxysilane (TEOS) in 1 mM sodium citrate (pH 7.2) containing 150 mM NaCl; the final protein and TEOS concentrations in the reaction mixture were 0.05 mg/ml and 150 mM, respectively. The reaction mixture was incubated at 37°C for 16 days without stirring.

To examine the progress of the sol–gel reaction of TEOS, an aliquot of the sample was analysed under a JEM-1210 electron microscope at 80 kV. Numerous silica

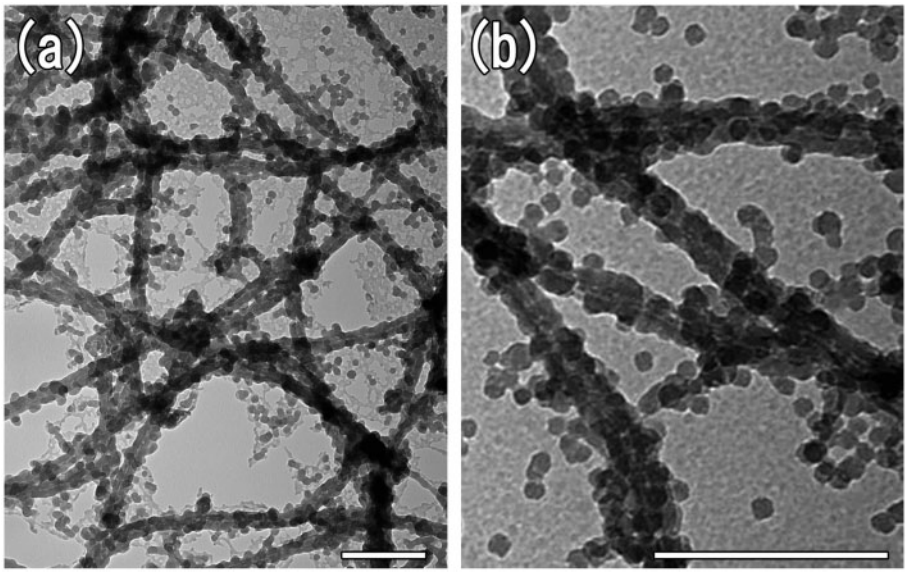

Fig. 2. **TEM images of the silica-coated vimentin IFs before calcination.** The sample was analysed without negative staining. The contrast between the dark outlines and the centrelines along the fibres indicates the hollow structure of the silica fibres. Scale bars represent 200 nm.

fibres with lengths of several micrometers and outer diameters of 35–55 nm were observed (Fig. 2); the contrast between the dark outlines and the centrelines indicates the hollow structure of the silica fibres. These results suggest that the sol-gel reaction of TEOS occurred preferentially on the surface of vimentin IFs and formed the silica-coated fibres. While it was previously reported that the thickness of silica coating on a template is related to the reaction time and TEOS concentration (*10*, *12*, *28*), we observed that higher concentrations of TEOS resulted in increased amorphous silica. When the final concentration of TEOS in the reaction mixture was reduced to 20 mM, fibres that were lightly coated with silica, but not thick enough to distinguish the inner and outer structures, were exclusively obtained (data not shown). Speculatively, the amorphous silica may have been produced, at least in part, by non-specific polymerization of TEOS or by polymerization of TEOS on the surface of vimentin oligomers that were unable to assemble further into IFs (Fig. 2).

An aliquot (~100 µl) of the reaction mixture was dried at 40°C for 1 day to obtain a powder of the silica/vimentin IF composites. The composites were heated at 200°C for 1 h and at 400°C for 2 h under a nitrogen atmosphere, and finally at 400°C for 2 h under aerobic conditions to remove IFs. The heating rate was 10°C per minute. The calcinated samples were suspended in milliQ water and dropped on specimen grids for TEM, then after 3 min the excess solution was drained by touching filter paper. TEM images of the samples after calcination at 400°C under a nitrogen atmosphere, and at 400°C under aerobic conditions can be seen in Fig. 3a and b–d, respectively. The image (a) was obtained under a JEM-1210 electron microscope at 80 kV and the images (b–d) under a JEM-2000FX electron microscope (JEOL) at 200 kV. The hollow silica nanotubes had an outer diameter of 35–55 nm and an average inner diameter of 10 nm, comparable to the diameter of vimentin IFs (Fig. 1a). Interestingly, the hollow silica nanotubes appeared to have a gnarled surface structure with an 18–26 nm repeating pattern, comparable to the 21-nm beading pattern along vimentin IFs (Fig. 1b and c) (*23*, *25–27*) These results suggest that the silica nanotubes largely replicated the characteristic morphology of vimentin IFs. However, no repeating patterns were evident in the inner structures of the silica nanotubes, which may relate to fusion of the silica directly contacting with the vimentin IFs during calcination.

In the present study, we demonstrated that vimentin IFs were able to be used as a template for the sol–gel polymerization of TEOS to produce hollow silica nanotubes. The head domain of vimentin might play a critical role in the specific polymerization of TEOS on the surface of vimentin IFs as the abundance of arginine residues, but only few acidic residues, causes the head domain of vimentin to be very basic (pI 11.6) and the rod and tail domains to be relatively acidic (pI, 4.5 and 5.0, respectively). The head domain of vimentin is considered to essentially lie on the surface of the IF structure (*16–18*). As such, the cationic charges of the head domain, possibly catalysing the hydrolysis of TEOS, can attract the negatively charged TEOS derivatives such as partially hydrolysed TEOS and TEOS oligomers to the surface of vimentin IFs at the pH we used (*3*, *4*, *6*). Then, polymerization of the TEOS derivatives concentrated around IFs proceeds. In addition, the head and the tail domains are considered responsible for the formation of the 21-nm beading pattern along the vimentin IFs due to their regular deposition on the filament surface (*16*, *17*, *23*). It is possible that the gnarled surface structure of the silica nanotubes observed in the present study was produced by replicating the beading pattern of vimentin IFs. Silica nanotubes prepared using collagen fibres as a template were reported to have a gnarled

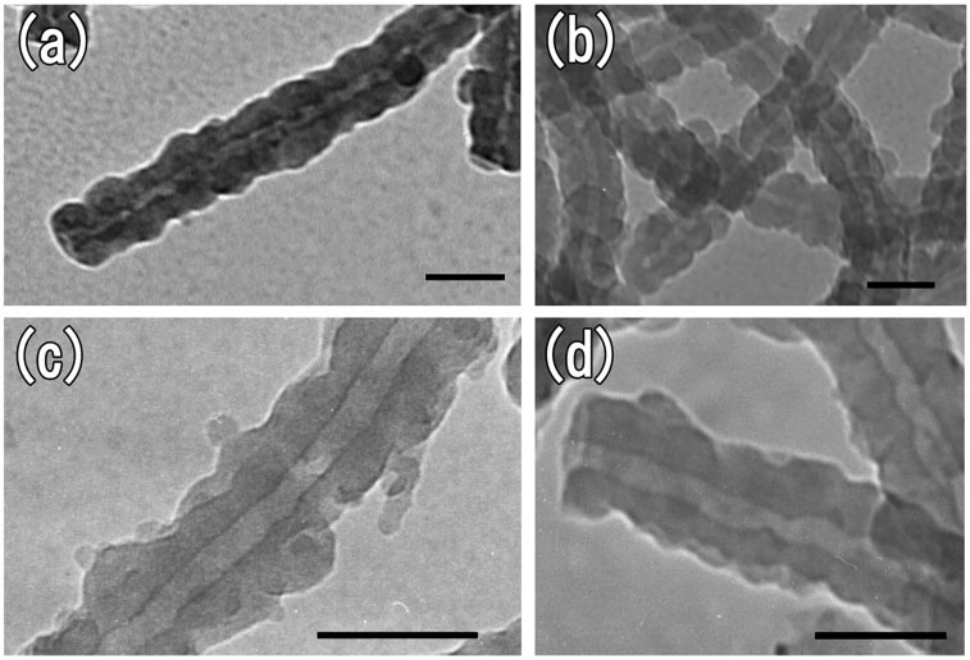

Fig. 3. **TEM images of the hollow silica nanotubes after calcination at 400°C under a nitrogen atmosphere (a) and at 400°C under aerobic conditions (b–d).** The hollow silica nanotubes exhibited a gnarled surface structure and an average inner diameter of 10 nm, comparable to the diameter of vimentin IFs. Scale bars represent 50 nm.

surface structure with 60–80-nm repeating pattern, comparable to that of the collagen groove (67 nm) (*10*). By contrast, relatively smooth surfaces were reported for silica nanotubes synthesized on peptide amphiphile nanofibre templates with smooth surfaces (*12*). The results from the present study support the concept that silica shells formed by the sol–gel polymerization of silica precursors replicate the surface structures of organic templates with high fidelity.

In summary, we demonstrated the application of vimentin IFs as a template for preparation of hollow silica nanotubes by sol–gel polymerization of TEOS, with excellent replication of the characteristic morphology of vimentin IFs into the hollow silica nanotubes. Future studies will focus on production of a more regulated and tailorable silica nanostructure, and on modification of IF templates such as parallel alignment of the filaments or construction of IF networks with lateral cross-bridges.

ACKNOWLEDGEMENTS

We thank Professor Y. Oishi for helpful discussion, and K. Nakao and T. Tabata for technical assistance and pertinent comments.

CONFLICT OF INTEREST

None declared.

REFERENCES

1. Xia, Y., Yang, P., Sun, Y., Wu, Y., Mayers, B., Gates, B., Yin, Y., Kim, F., and Yan, C. (2003) One-dimensional nanostructures: Synthesis, characterization, and applications. *Adv. Mater.* **15**, 353–389
2. Remskar, M. (2004) Inorganic nanotubes. *Adv. Mater.* **16**, 1497–1504
3. Soler-Illia, G.J.d.A.A., Sanchez, C., Lebeau, B., and Patarin, J. (2002) Chemical strategies to design textured materials: from microporous and mesoporous oxides to nanonetworks and hierarchical structures. *Chem. Rev.* **102**, 4093–4138
4. Caruso, R.A. and Antonietti, M. (2001) Sol−gel nanocoating: an approach to the preparation of structured materials. *Chem. Mater.* **13**, 3272–3282
5. Estroff, L.A. and Hamilton, A.D. (2001) At the interface of organic and inorganic chemistry: bioinspired synthesis of composite materials. *Chem. Mater.* **13**, 3227–3235
6. van Bommel, K.J.C., Friggeri, A., and Shinkai, S. (2003) Organic templates for the generation of inorganic materials. *Angew. Chem. Int. Ed.* **42**, 980–999
7. Baral, S. and Schoen, P. (1993) Silica-deposited phospholipid tubules as a precurosor to hollow submicron-diameter silica cylinders. *Chem. Mater.* **5**, 145–147
8. Ji, Q., Iwaura, R., Kogiso, M., Jung, J.H., Yoshida, K., and Shimizu, T. (2004) Direct sol−gel replication without catalyst in an aqueous gel system: from a lipid nanotube with a single bilayer wall to a uniform silica hollow cylinder with an ultrathin wall. *Chem. Mater.* **16**, 250–254
9. Adachi, M., Harada, T., and Harada, M. (1999) Formation of huge length silica nanotubes by a templating mechanism in the laurylamine/tetraethoxysilane system. *Langmuir* **15**, 7097–7100
10. Ono, Y., Kanekiyo, Y., Inoue, K., Hojo, J., Nango, M., and Shinkai, S. (1999) Preparation of novel hollow fiber silica using collagen fibers as a template. *Chem. Lett.* **28**, 475–476
11. Numata, M., Sugiyasu, K., Hasegawa, T., and Shinkai, S. (2004) Sol–gel reaction using DNA as a template: an attempt toward transcription of DNA into inorganic materials. *Angew. Chem. Int. Ed.* **43**, 3279–3283
12. Yuwono, V.M. and Hartgerink, J.D. (2007) Peptide amphiphile nanofibers template and catalyze silica nanotube formation. *Langmuir* **23**, 5033–5038

13. Meegan, J.E., Aggeli, A., Boden, N., Brydson, R., Brown, A.P., Carrick, L., Brough, A.R., Hussain, A., and Ansell, R.J. (2004) Designed self-assembled beta-sheet peptide fibrils as templates for silica nanotubes. *Adv. Funct. Mater.* **14**, 31–37
14. Khanal, A., Inoue, Y., Yada, M., and Nakashima, K. (2007) Synthesis of silica hollow nanoparticles templated by polymeric micelle with core–shell–corona structure. *J. Am. Chem. Soc.* **129**, 1534–1535
15. Inagaki, M., Matsuoka, Y., Tsujimura, K., Ando, S., Tokui, T., Takahashi, T., and Inagaki, N. (1996) Dynamic property of intermediate filaments: regulation by phosphorylation. *BioEssays* **18**, 481–487
16. Parry, D.A. and Steinert, P.M. (1999) Intermediate filaments: molecular architecture, assembly, dynamics and polymorphism. *Q. Rev. Biophys.* **32**, 99–187
17. Herrmann, H. and Aebi, U. (2004) Intermediate filaments: molecular structure, assembly mechanism, and integration into functionally distinct intracellular scaffolds. *Annu. Rev. Biochem.* **73**, 749–789
18. Parry, D.A., Strelkov, S.V., Burkhard, P., Aebi, U., and Herrmann, H. (2007) Towards a molecular description of intermediate filament structure and assembly. *Exp. Cell Res.* **313**, 2204–2216
19. Steinert, P.M., Cantieri, J.S., Teller, D.C., Lonsdale-Eccles, J.D., and Dale, B.A. (1981) Characterization of a class of cationic proteins that specifically interact with intermediate filaments. *Proc. Natl Acad. Sci. USA* **78**, 4097–4101
20. Rao, M.V., Campbell, J., Yuan, A., Kumar, A., Gotow, T., Uchiyama, Y., and Nixon, R.A. (2003) The neurofilament middle molecular mass subunit carboxyl-terminal tail domains is essential for the radial growth and cytoskeletal architecture of axons but not for regulating neurofilament transport rate. *J. Cell Biol.* **163**, 1021–1031
21. Aebi, U., Cohn, J., Buhle, L., and Gerace, L. (1986) The nuclear lamina is a meshwork of intermediate-type filaments. *Nature* **323**, 560–564
22. Szeverenyi, I., Cassidy, A.J., Chung, C.W., Lee, B.T., Common, J.E., Ogg, S.C., Chen, H., Sim, S.Y., Goh, W.L., Ng, K.W., Simpson, J.A., Chee, L.L., Eng, G.H., Li, B., Lunny, D.P., Chuon, D., Venkatesh, A., Khoo, K.H., McLean, W.H., Lim, Y.P., and Lane, E.B. (2008) The human intermediate filament database: comprehensive information on a gene family involved in many human diseases. *Hum. Mutat.* **29**, 351–360
23. Ando, S., Nakao, K., Gohara, R., Takasaki, Y., Suehiro, K., and Oishi, Y. (2004) Morphological analysis of glutaraldehyde-fixed vimentin intermediate filaments and assembly-intermediates by atomic force microscopy. *Biochim. Biophys. Acta* **1702**, 53–65
24. Bradford, M.M. (1976) A rapid and sensitive method for the quantitation of microgram quantities of protein utilizing the principle of protein-dye binding. *Anal. Biochem.* **72**, 248–254
25. Henderson, D., Geisler, N., and Weber, K. (1982) A periodic ultrastructure in intermediate filaments. *J. Mol. Biol.* **155**, 173–176
26. Milam, L. and Erickson, H.P. (1982) Visualization of a 21-nm axial periodicity in shadowed keratin filaments and neurofilaments. *J. Cell Biol.* **94**, 592–596
27. Ip, W., Hartzer, M.K., Pang, Y.Y., and Robson, R.M. (1985) Assembly of vimentin *in vitro* and its implications concerning the structure of intermediate filaments. *J. Mol. Biol.* **183**, 365–375
28. Yin, Y., Lu, Y., Sun, Y., and Xia, Y. (2002) Silver nanowires can be directly coated with amorphous silica to generate well-controlled coaxial nanocables of silver/silica. *Nano Lett.* **2**, 427–430